PHYSICAL REVIEW B **78**, 121303(R) (2008)

Co_2FeSi/GaAs/(Al,Ga)As spin light-emitting diodes: Competition between spin injection and ultrafast spin alignment

M. Ramsteiner,[*] O. Brandt, T. Flissikowski, H. T. Grahn, M. Hashimoto,[†] J. Herfort, and H. Kostial
Paul-Drude-Institut für Festkörperelektronik, Hausvogteiplatz 5-7, 10117 Berlin, Germany

(Received 24 July 2008; published 18 September 2008)

Electrical injection from the Heusler alloy Co_2FeSi into (Al,Ga)As is investigated for different growth temperatures T_G of the injector layer. Depending on T_G, the spin polarization of injected electrons in the semiconductor is determined by two competing mechanisms: actual spin injection at the Co_2FeSi/(Al,Ga)As interface and ultrafast spin alignment in the (Al,Ga)As layer. This layer is strongly affected by the thermally activated diffusion of Co, Fe, and Si during the growth of the Co_2FeSi layers. Despite the electrical compensation and magnetic transformation in the underlying semiconductor structure, a spin-injection efficiency of at least 50% is achieved as deduced from the analysis of electroluminescence and time-resolved photoluminescence data.

DOI: 10.1103/PhysRevB.78.121303 PACS number(s): 72.25.Hg, 72.25.Dc, 72.25.Mk, 72.25.Rb

Spin injection from ferromagnetic metals into semiconductors is an important building block for spintronic applications.[1–4] With respect to the desired high spin-injection efficiency, a very promising concept is the introduction of a spin-dependent tunnel barrier between the ferromagnetic injector and the semiconductor as demonstrated recently for the system (Co,Fe)/MgO/(Al,Ga)As.[5,6] Assuming perfect spin filtering by the tunnel barrier, a 100% spin-injection efficiency can in principle be achieved. An alternative approach is to utilize a halfmetal as spin-injector material. In this case, the complete spin polarization of electrons at the Fermi energy necessarily leads to a spin-injection efficiency of 100% without the need for a tunnel barrier acting as a spin filter. In this respect, ferromagnetic Heusler alloys are of particular interest due to the fact that some of them have been predicted to be halfmetallic. For one member of this material class, Co_2MnGe, spin injection into (Al,Ga)As has been investigated.[7] However, the spin-injection efficiency has been limited to relatively low values due to the formation of a disordered phase at the interface with the semiconductor. The Heusler alloy Co_2FeSi is also predicted to be a halfmetal and has the advantage to be closely lattice matched to GaAs allowing for the synthesis of high-quality epitaxial layers on GaAs/(Al,Ga)As spin light-emitting diodes (spin LEDs).

In this Rapid Communication, we investigate the spin injection from Co_2FeSi in GaAs/(Al,Ga)As spin LEDs. The spin LEDs with a design similar to that given in Ref. 4 (cf. Table I) were grown in a dual-chamber molecular-beam epitaxy (MBE) system. These devices comprise the following layer sequence grown in the semiconductor-MBE chamber on p-type GaAs(001) substrates: 400 nm p-GaAs ($p=1\times10^{17}$ cm^{-3}), 200 nm p-$Al_{0.1}Ga_{0.9}As$ ($p=1\times10^{16}$ cm^{-3}), 50 nm of undoped material containing a 10-nm-thick GaAs quantum well sandwiched between 20-nm-thick $Al_{0.1}Ga_{0.9}As$ barriers, 115 nm n-$Al_{0.1}Ga_{0.9}As$ (100 nm with $n=1\times10^{16}$ cm^{-3} and 15 nm linearly graded from $n=1\times10^{16}$ to 5×10^{18} cm^{-3}), and 15–25 nm n-$Al_{0.1}Ga_{0.9}As$ ($n=5\times10^{18}$ cm^{-3}). After the growth of the semiconductor structure, the samples were transferred to the metal-MBE growth chamber in ultrahigh vacuum, and a 9-nm-thick Co_2FeSi layer was deposited at temperatures of 100 °C (LED 1 and LED 1a), 200 °C (LED 2), and 300 °C (LED 3). For more details about the Co_2FeSi growth, we refer the readers to Ref. 8. The MBE-grown structures were subsequently processed into mesa-shaped devices with a diameter of 450 μm. The electroluminescence (EL) measurements were performed in Faraday geometry with the LEDs placed in a superconducting magnet system. The circular polarization degree of the EL signal was analyzed by using a photoelastic modulator (PEM) in combination with lock-in detection. The degree of circular polarization is determined by $P=(I_+-I_-)/(I_++I_-)$, where I_+ (I_-) is the intensity of right (left) circularly polarized light. The absolute value of the polarization degree P is identical to the spin polarization of the radiatively recombining electrons if the heavy holes are assumed to be unpolarized. Time-resolved photoluminescence (PL) measurements were performed using a synchro-scan streak camera system

TABLE I. Co_2FeSi-growth temperature T_G, postgrowth thermal annealing temperature T_A, injector material (Co_2FeSi or Ti), and type of magnetic-field dependence in a spin-injection experiment (PM =paramagnetic or FM=ferromagnetic) for the spin LEDs under investigation.

	LED 1	LED 2	LED 3	LED 1a	LED 2t	LED 3t
T_G (°C)	100	200	300	100	200	300
T_A (°C)	—	—	—	300	—	—
Injector	Co_2FeSi	Co_2FeSi	Co_2FeSi	Co_2FeSi	Ti	Ti
Type	—	PM	FM	FM	PM	—

 ©2008 The American Physical Society

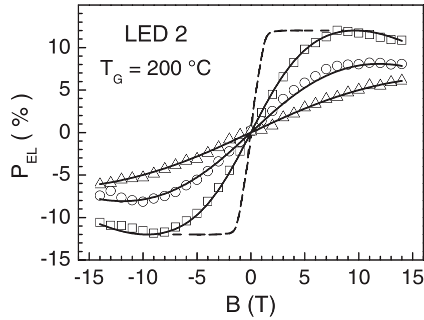

FIG. 1. Degree of circular EL polarization P_{EL} as a function of external magnetic field of LED 2 at 20 K (squares), 50 K (circles), and 100 K (triangles) together with the out-of-plane magnetization curve measured by SQUID (dashed line in arbitrary units) and the expected polarization for a paramagnetic DMS (solid lines) according to a model based on Eqs. (1) and (2).

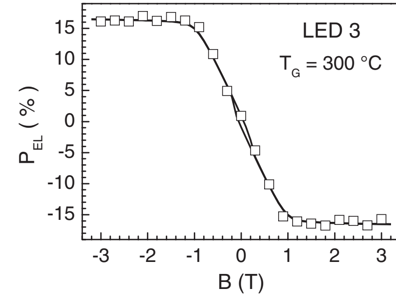

FIG. 2. Degree of circular EL polarization P_{EL} as a function of external magnetic field at 20 K of LED 3 (squares) together with the out-of-plane magnetization curve measured by SQUID (solid line in arbitrary units). For a better comparison with the EL polarization, the sign of the magnetization curve has been reversed with respect to that in Fig. 1.

in conjunction with a Ti:sapphire laser emitting 200 fs pulses with a repetition rate of 76 MHz. An initial spin polarization of photoexcited carriers was created by pump pulses, which were right circularly polarized by means of a quarter-wave plate. The emitted PL light was analyzed into its right (I_{++}) and left (I_{+-}) circularly polarized components.

Investigations of $Co_2FeSi/GaAs$ structures by transmission electron microscopy (TEM) as described in Ref. 9 revealed interfacial reactions at growth temperatures $T_G > 250$ °C with the conclusion that $T_G \sim 200$ °C is optimal for achieving high spin-injection efficiency from Co_2FeSi into GaAs. However, the investigated LEDs exhibit variations in their electro-optical characteristics wider than expected from the structural data obtained by the TEM study.[9] In particular, the EL intensity of LED 1 is too weak to determine its polarization. In contrast, the EL intensity of LEDs with higher Co_2FeSi growth temperature is several orders of magnitude higher, but their polarization properties are strikingly different. The EL polarization (P_{EL}) of LED 2 is shown in Fig. 1 as a function of the external magnetic field. P_{EL} of this device does not follow the out-of-plane magnetization of the Co_2FeSi injector measured by superconducting quantum interference device (SQUID) magnetometry (shown in Fig. 1 as dashed line in arbitray units and with the sign selected according to that of P_{EL}), from which a saturation at an external magnetic field of about 1 T is expected. Instead, the saturation of P_{EL} at 20 K requires a field as high as 8 T, which resembles the magnetic response of a paramagnetic material, such as a dilute magnetic semiconductor (DMS).

In contrast, the EL polarization of LED 3 clearly evidences a ferromagnetic response since it tracks the magnetization of the injector material over the whole range of magnetic fields as shown in Fig. 2 (note the different scale compared to Fig. 1). A further striking difference between LEDs 3 and 2 is the opposite sign of P_{EL}. Thermal annealing of LED 1 for 30 min at 300 °C (LED 1a in Table I) results in an EL intensity and a polarization response basically identical to the one of LED 3. It is important to note that the observed polarization degrees of 15% to 20% in the saturation range are basically one order of magnitude larger as compared to our previous spin-injection experiments using Fe, Fe_3Si, or MnAs injectors.[1,10,11]

The complex behavior evidenced by Figs. 1 and 2 is elucidated by secondary-ion mass spectrometry (SIMS) and TEM. Figure 3 displays the SIMS depth profiles for Co [Fig. 3(a)], Fe [Fig. 3(b)], and Si [Fig. 3(c)] in spin LEDs onto which a Co_2FeSi injector was deposited at T_G=100 °C, 200 °C, and 300 °C. Note that the injector layer has been removed by selective wet chemical etching withHF prior to the SIMS depth profiling. The concentration of all elements in the upper $Al_{0.1}Ga_{0.9}As$ layer, but particularly of Co and Fe, is seen to increase drastically with increasing T_G. For T_G =300 °C, the concentration of both Co and Fe exceeds several 10^{20} cm^{-3} in the topmost 20 nm of the LED structure. For the case of Fe, an Arrhenius plot of the integrated concentration yields an activation energy of 0.44 eV, while the diffusion of Co seems to be more complex and cannot be

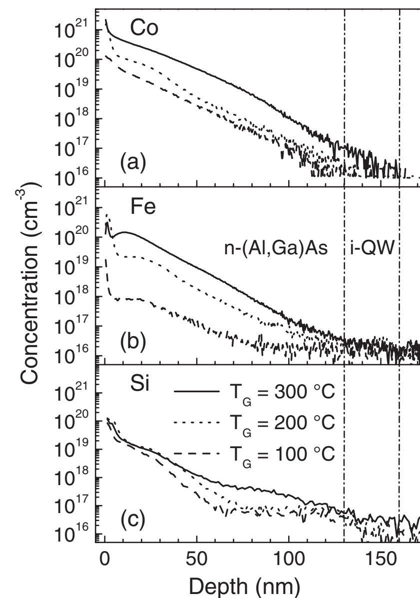

FIG. 3. Concentration depth profiles of (a) Co, (b) Fe, and (c) Si in LEDs with Co_2FeSi injectors grown at T_G=300 °C (solid curves), T_G=200 °C (dotted curves), and T_G=100 °C (dashed curves) measured by secondary-ion mass spectrometry (SIMS). The vertical dash-dotted lines indicate the intrinsic region of the LED structures (i-QW).

described by a simple activated process. Finally, the SIMS profiles of LED 1a (cf. Table I) reveal that postgrowth thermal annealing at 300 °C does not induce significant diffusion into the semiconductor structure (not shown here).

SIMS integrates over an area of typically $60 \times 60\ \mu m^2$ and thus does not give information about the actual lateral distribution of the diffused species. As mentioned above, previous TEM experiments in conjunction with x-ray diffraction have revealed the formation of (Co,Ga)As precipitates at growth temperatures above 250 °C.[9] At lower temperatures, no precipitates were found suggesting that both Co and Fe are incorporated as isolated impurities, which are expected to be electrically active.

With the help of these additional experiments, we are in a position to suggest a tentative yet comprehensive model for the explanation of our results. At T_G=100 °C, we suppose that nonradiative defects are generated at the $Co_2FeSi/Al_{0.1}Ga_{0.9}As$ interface and remain there due to their insufficient mobility at this low temperature. Consequently, the EL efficiency of LED 1 is very low. At T_G=200 °C, these nonradiative defects are presumably annihilated by diffusion at the interface. However, significant diffusion of Co and Fe sets in simultaneously, effectively converting the upper $Al_{0.1}Ga_{0.9}As$ layer into a DMS with paramagnetic response. Finally, at T_G=300 °C, bulk segregation of Co and Fe occurs causing the formation of precipitates and the depletion of Co and Fe from the DMS matrix, which is very similar to the behavior reported for Fe in GaAs.[12,13] This process effectively depletes the matrix of substitutional Co and Fe.

The observed saturation of the polarization at 8 T for LED 2 (cf. Fig. 1) is a signature of spin alignment in a paramagnetic semiconductor. Consequently, spin alignment in the upper $Al_{0.1}Ga_{0.9}As$ barrier has to be taken into account. We thus expect the following magnetic-field dependence of P_{EL} in thermal equilibrium:[14]

$$P_{EL}(B) = \tanh\left[\frac{g\mu_B(B + B_{int})}{2k_B T}\right], \qquad (1)$$

where k_B is the Boltzmann factor and T is the temperature. $\Delta E(B) = g\mu_B B$ is the energy separation between the Zeeman sublevels of electrons in the upper $Al_{0.1}Ga_{0.9}As$ barrier in an external magnetic field B. For a magnetic semiconductor, we have to consider the additional splitting $\Delta E_{int}(B) = g\mu_B B_{int}$ generated by the internal field produced by the magnetic atoms given by

$$B_{int} = \frac{N_0 \alpha x J}{g\mu_B} B_J\left(\frac{g_M \mu_B J B}{k_B T}\right), \qquad (2)$$

where g_M is the g factor, J is the total angular-momentum quantum number, and x is the concentration of magnetic atoms. $N_0\alpha$ is the exchange constant and $B_J(B,T)$ is the Brillouin function. We analyze the data with a rate-equation model, which takes into account spin scattering, such that thermal equilibrium according to Eq. (1) is reached when the spin-relaxation time is much shorter than the transit time of the electrons through the upper $Al_{0.1}Ga_{0.9}As$ barrier.[15] Furthermore, our model assumes a generation term, which corresponds to spin injection with a magnetic-field dependence according to the ferromagnetic out-of-plane magnetization of Co_2FeSi. Indeed, the magnetic-field dependence in Fig. 1 can be described very well by our model using a spin-relaxation time about two orders of magnitude shorter than the transit time. Since the transit time is expected to be on the order of picoseconds, this finding constitutes an ultrafast spin alignment. For the remaining parameters in Eqs. (1) and (2), we assume values which are typical for GaAs-based DMS.[15] The observed temperature dependence between 20 and 100 K is characteristic for a paramagnetic DMS and can be simulated consistently with our DMS-related model (cf. Fig. 1; for details see Ref. 15) The sign of P_{EL} due to spin alignment depends on the sign of the g factors of free electrons and holes in the semiconductor structure. These signs and, exclusively for a DMS, the sign of the exchange constant $N_0\alpha$ define the ordering of the Zeeman levels. We verified that the spin alignment due to Zeeman thermalization in LEDs without ferromagnetic injector leads to the opposite sign of P_{EL} as compared to that of LED 2. The corresponding contribution to P_{EL} from Zeeman thermalization inside or below the active region is observed in Fig. 1 for T=20 K at very large magnetic fields as a slight decrease of P_{EL}. Thus, the observed sign of P_{EL} strongly supports our model.

The experimental observation for LED 3 (cf. Fig. 2) provides evidence for spin injection from Co_2FeSi with the preferential spin orientation opposite to that in thermal equilibrium in the DMS-like $Al_{0.1}Ga_{0.9}As$ barrier of LED 2. This result is explained by the effective depletion of the upper $Al_{0.1}Ga_{0.9}As$ barrier of substitutional Co and Fe so that spin alignment is rendered ineffective. Our model is confirmed by the results obtained from LEDs after the replacement of the Co_2FeSi injectors by a nonmagnetic Ti injector. After the exchange of a Co_2FeSi injector grown at 300 °C (LED 3t in Table I) neither paramagnetic nor ferromagnetic behavior is obtained. On the contrary, after removal of a Co_2FeSi injector grown at 200 °C (LED 2t in Table I) we still observe a clear paramagnetic signature with the absolute value of P_{EL} remaining nearly unchanged. The situation for Co_2FeSi growth at 200 °C is particularly interesting, since spin injection from ferromagnetic Co_2FeSi presumably coexists with the competing ultrafast spin alignment in the underlying paramagnetic semiconductor. In order to explain the complete absence of a remaining ferromagnetic signature in the EL polatization (cf. Fig. 1), we have to assume a very strong spin scattering in the topmost $Al_{0.1}Ga_{0.9}As$ layer leading to a complete relaxation of spins into thermal equilibrium as given by Eq. (1). Considering the large concentration of magnetic impurities in that layer, this strong spin scattering is not surprising.

Another interesting point we would like to stress is the high EL polarization measured for LED 1a. Apparently, the annealing effectively removes nonradiative defects but does not induce a diffusion of Co and Fe into the semiconductor. Consequently, MBE growth at low temperatures combined with postgrowth annealing seems to be a potentially attractive strategy to produce efficient spin-injection devices without strong interdiffusion at the ferromagnet/semiconductor interface.

For obtaining the actual spin-injection efficiency S at the

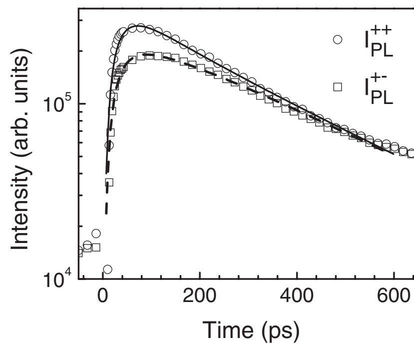

FIG. 4. Right (circles: I_{++}) and left (squares: I_{+-}) circularly polarized PL transients of the reference sample upon right circularly polarized excitation in the barrier at 20 K. The lines indicate the simultaneous fit of the data by the model mentioned in the text.

ferromagnet/semiconductor interface, we examine the carrier recombination and spin dynamics in the active region of our spin LEDs.[10] For this aim, we perform time-resolved PL on a reference *n*-*i*-*n* structure with an active region identical to that of the spin LEDs under investigation. Figure 4 shows the right and left circularly polarized PL transients from this sample for excitation at an energy above the band gap of the $Al_{0.1}Ga_{0.9}As$ barriers at 20 K. We analyzed the data with a model which takes into account not only the spin flip of excitons (τ_x) but also the spin flip of electrons (τ_e) and holes (τ_h) and thus the participation of dark exciton states.[16] A simultaneous fit of the data for both polarizations by this model (cf. Fig. 4) yields $\tau_x=250$, $\tau_e=800$, $\tau_h=20$, and the radiative lifetime $\tau_r=150$ ps. With these values, the measured circular polarization P_{EL} of 17% corresponds to an actual value for S of 51%. While this value is lower than the desired one (100%), one has to bear in mind the efficient scattering of spin-polarized electrons by the magnetic impurities in the upper $Al_{0.1}Ga_{0.9}As$ layer as mentioned above. This scattering reduces the initial spin polarization of the electrons prior to their capture by the GaAs quantum well. Therefore, the value deduced for S is still a lower limit for the actual spin-injection efficiency at the ferromagnet/semiconductor interface. This result leaves us with the open question of whether or not Co_2FeSi is indeed a halfmetallic spin injector. In this context, it is interesting to note that the sign of P_{EL} observed for LED 3 (cf. Fig. 2) is opposite to that of our previous spin-injection experiments using Fe, Fe_3Si, or MnAs injectors[1,10,11] reflecting a qualitatively different electronic band structure in Co_2FeSi.

Finally, let us stress that the diffusion of Co and Fe not only leads to a *magnetic* modification of the topmost semiconductor part in our spin LEDs but also to an *electrical* one. Since both Co and Fe are deep acceptors in (Al,Ga)As and are both present in very large concentrations (cf. Fig. 3), the topmost $Al_{0.1}Ga_{0.9}As$ layer in our LEDs is unlikely to be *n* type as intended but is probably entirely compensated by the huge concentration of deep acceptors present in the material. Thus, the topmost layer is expected to be depleted, which is actually confirmed by capacitance-voltage measurements (not shown here). Consequently, the formation of a Schottky barrier at the ferromagnet/semiconductor interface cannot take place, and tunneling should not play a significant role for the injection process. At the same time, we observe a rather large spin-injection efficiency, which casts doubt onto the common belief that tunneling is a prerequisite for spin injection from a metal into a semiconductor.

In summary, we have studied the electrical injection from the Heusler alloy Co_2FeSi into (Al,Ga)As. The magnetic and electrical properties of the semiconductor part in the investigated spin LEDs have been found to be strongly modified by thermally activated diffusion during MBE growth. The corresponding polarization of the EL reflects the competing mechanisms of spin injection and ultrafast spin alignment. Despite the strong diffusion of magnetic acceptor species, a large spin-injection efficiency of at least 50% has been achieved. Our results demonstrate the potential of Co_2FeSi for being a halfmetallic spin injector and indicate that tunneling is not necessarily an important process for spin injection at metal/semiconductor interfaces.

We acknowledge expert technical assistance by Edith Wiebicke and Gerd Paris as well as comments and a careful reading of the manuscript by Paulo Santos.

*ramsteiner@pdi-berlin.de

†Present address: Department of Electrical and Computer Engineering, University of California, Santa Barbara, CA 93106, USA.

[1] H. J. Zhu *et al.*, Phys. Rev. Lett. **87**, 016601 (2001).
[2] A. T. Hanbicki *et al.*, Appl. Phys. Lett. **80**, 1240 (2002).
[3] V. F. Motsnyi *et al.*, Phys. Rev. B **68**, 245319 (2003).
[4] C. Adelmann *et al.*, Phys. Rev. B **71**, 121301(R) (2005).
[5] X. Jiang *et al.*, Phys. Rev. Lett. **94**, 056601 (2005).
[6] R. Wang *et al.*, Appl. Phys. Lett. **86**, 052901 (2005).
[7] X. Y. Dong *et al.*, Appl. Phys. Lett. **86**, 102107 (2005).
[8] M. Hashimoto *et al.*, J. Appl. Phys. **98**, 104902 (2005).
[9] M. Hashimoto *et al.*, J. Vac. Sci. Technol. B **25**, 1453 (2007).
[10] M. Ramsteiner *et al.*, Phys. Rev. B **66**, 081304(R) (2002).
[11] A. Kawaharazuka *et al.*, Appl. Phys. Lett. **85**, 3492 (2004).
[12] S. Hirose *et al.*, Thin Solid Films **371**, 272 (2000).
[13] R. Moriya *et al.*, Physica E (Amsterdam) **10**, 224 (2001).
[14] W. Heimbrodt *et al.*, Physica E (Amsterdam) **10**, 175 (2001).
[15] O. Brandt *et al.* (unpublished).
[16] M. Z. Maialle *et al.*, Phys. Rev. B **47**, 15776 (1993).